



HAL
open science

High order stabilized finite element method for MHD plasma modeling

J Tarcisio-Costa, Boniface Nkonga

► **To cite this version:**

J Tarcisio-Costa, Boniface Nkonga. High order stabilized finite element method for MHD plasma modeling . ICOSAHOM 2016 - International Conference On Spectral and High Order Methods, Jun 2016, Rio de Janeiro, Brazil. hal-01426950

HAL Id: hal-01426950

<https://inria.hal.science/hal-01426950>

Submitted on 5 Jan 2017

HAL is a multi-disciplinary open access archive for the deposit and dissemination of scientific research documents, whether they are published or not. The documents may come from teaching and research institutions in France or abroad, or from public or private research centers.

L'archive ouverte pluridisciplinaire **HAL**, est destinée au dépôt et à la diffusion de documents scientifiques de niveau recherche, publiés ou non, émanant des établissements d'enseignement et de recherche français ou étrangers, des laboratoires publics ou privés.

High order stabilized finite element method for MHD plasma modeling

J. Tarcisio-Costa, B.Nkonga
`jose.costa@inria.fr`

ICOSAHOM - Rio de Janeiro June, 28th 2016

- 1 Introduction
- 2 Stabilization for Full MHD
- 3 Applications: Internal kink, Bohm B.C.
- 4 Conclusions and perspectives

Motivations

- Go from Reduced to the full MHD model
- Ensure stability of flows dominated by convection
- Boundary conditions

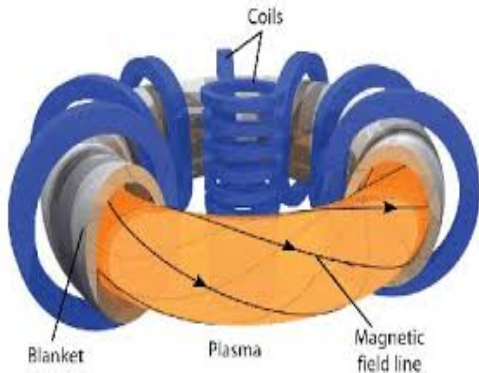
Main goal: use JOREK to simulate Edge-localized modes (ELMS) with the Full-MHD model

Tokamaks

- Tokamak stands for: Toroidal chamber with magnetic coils (From Russian: Toroidal'naya Kamera s Magnitnymi Katushhami).
- Principal tokamaks at present: JET (UK), Asdex-Upgrade (Germany), Tore-Supra (France) and DIII-D (USA)
- Drifts → Nested magnetic field lines → Confinement is improved
- The amplification factor of a fusion reactor is defined as

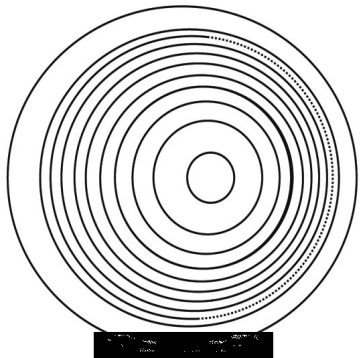
$$Q = \frac{P_{fus}}{P_{inj}}$$

- JET: $Q \approx 1$ - ITER: $Q = 10$
- Economically exploitable $Q = 50$



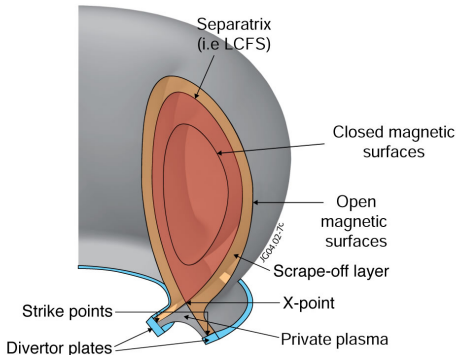
Tokamak configurations

There are two main configurations for tokamaks



Limiter

Material structure into the plasma



Divertor

X-point configuration
Material structure placed outside

- Nonlinear reduced MHD and full MHD under implementation
- Cubic C1 finite elements (quadrangles)/Fourier (modal)
- Galerkin formulation
- Linearized Crank-Nicholson and Gear: Implicit scheme
- GMRES solver, Hybrid paralelization (MPI/OpenMPI)

- Spatial discretization: 4th-order accurate Galerkin method based on Bézier Formalism
- An arbitrary quantity is expanded on a unit square as

$$P(s, t) = \sum_{i=1}^4 \sum_{j=1}^4 p_{ij} \sigma_{ij} b_{ij}(s, t)$$

- $(s, t) \in [0, 1]$, σ assure continuity of P
- Basis functions b_{ij} : Bernstein polynomials

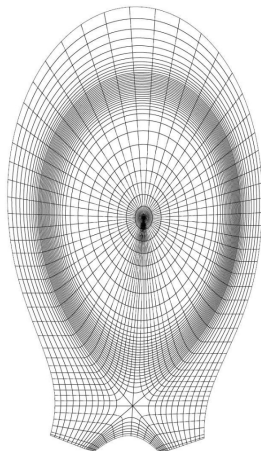
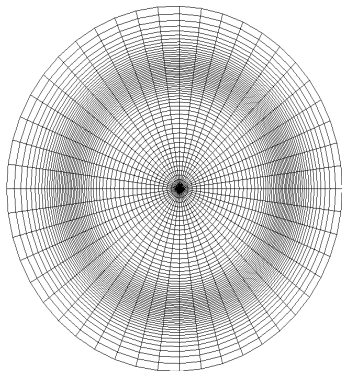
$$b_{11} = (1-s)^2(1-t)^2(1+2s)(1+2t),$$

$$b_{12} = 3(1-s)^2(1-t)^2(1+2t)s,$$

$$b_{13} = 3(1-s)^2(1-t)^2(1+2s)t,$$

$$b_{14} = 9(1-s)^2(1-t)^2st.$$

Examples of meshes: poloidal and X-point



System of equations: Full MHD

The single-fluid full MHD system in consideration is

$$\left\{ \begin{array}{l} \frac{\partial \rho}{\partial t} + \nabla \cdot \mathbf{m} = \nabla \cdot (\underline{\mathcal{D}} \nabla \rho'), \\ \frac{\partial \mathbf{m}}{\partial t} + \nabla \cdot \left(\frac{\mathbf{m} \otimes \mathbf{m}}{\rho} - \mathbf{B} \otimes \mathbf{B} \right) + \nabla \cdot \left(\rho + \frac{\mathbf{B} \cdot \mathbf{B}}{2} \right) = \nabla \cdot \underline{\boldsymbol{\tau}}, \\ \frac{\partial \mathcal{E}}{\partial t} + \nabla \cdot \left(\left(\mathcal{E} + \rho + \frac{\mathbf{B} \cdot \mathbf{B}}{2} \right) \frac{\mathbf{m}}{\rho} - \frac{\mathbf{B} \cdot \mathbf{m}}{\rho} \mathbf{B} \right) = \nabla \cdot \mathbf{q} + \nabla \cdot \left(\frac{\underline{\boldsymbol{\tau}} \mathbf{m}}{\rho} \right), \\ \frac{\partial \mathbf{B}}{\partial t} + \nabla \cdot \left(\frac{\mathbf{m} \otimes \mathbf{B} - \mathbf{B} \otimes \mathbf{m}}{\rho} \right) = -\nabla \times (\mathbf{E} + \mathbf{v} \times \mathbf{B}) \end{array} \right.$$

with $\mathbf{m} \equiv \rho \mathbf{v}$, $\mathcal{E} = \rho \varepsilon + \frac{1}{2\rho} \mathbf{m} \cdot \mathbf{m} + \frac{\mathbf{B} \cdot \mathbf{B}}{2}$, $\rho = (\gamma - 1) \rho \varepsilon = \rho T$,

$\mathbf{E} + \mathbf{v} \times \mathbf{B} = \underline{\boldsymbol{\eta}} \mathbf{J}$, $\mathbf{J} \equiv \nabla \times \mathbf{B}$.

The ideal MHD system driving the previous system can be written in the following compact form

$$\frac{\partial \mathbf{w}}{\partial t} + \nabla \cdot \underline{\mathbf{f}} = 0,$$

where

$$\mathbf{w} = \begin{pmatrix} \rho \\ \mathbf{m} \\ \mathcal{E} \\ \mathbf{B} \end{pmatrix}, \quad \underline{\mathbf{f}} = \begin{pmatrix} \mathbf{m}^T \\ \mathbf{v} \otimes \mathbf{m} + P\mathbb{I} - \mathbf{B} \otimes \mathbf{B} \\ \mathcal{H}\mathbf{m}^T - (\mathbf{B} \cdot \mathbf{v})\mathbf{B}^T \\ \mathbf{v} \otimes \mathbf{B} - \mathbf{B} \otimes \mathbf{v} \end{pmatrix}$$

$$P = p + \frac{\mathbf{B} \cdot \mathbf{B}}{2}, \quad \mathcal{H} = \frac{\mathcal{E} + P}{\rho}$$

Quasi-linear form

$$\frac{\partial \mathbf{w}}{\partial t} + \underline{\mathbf{L}}(\mathbf{w}, \partial) \mathbf{w} = 0$$

The operator $\underline{\mathbf{L}}(\mathbf{w}, \partial)$

$$\underline{\mathbf{L}}(\mathbf{w}, \partial) = \begin{pmatrix} 0 & \partial^T & 0 & \mathbf{0}^T \\ -\frac{\mathbf{m}}{\rho^2} \mathbf{m} \cdot \partial + \frac{\partial P}{\partial \rho} \partial & \frac{1}{\rho} (\mathbf{m} \otimes \partial + \mathbf{m} \cdot \partial) + \left(\frac{\partial P}{\partial \mathbf{m}} \otimes \mathbf{m} \right)^T & \frac{\partial P}{\partial \mathcal{E}} \partial & (\mathbf{B} \otimes \partial)^T - \mathbf{B} \cdot \partial + \left(\frac{\partial P}{\partial \mathbf{B}} \otimes \mathbf{m} \right)^T \\ \frac{\partial \mathcal{H}}{\partial \rho} \mathbf{m} \cdot \partial + \frac{\mathbf{B} \cdot \mathbf{m}}{\rho^2} \mathbf{B} \cdot \partial & \left(\frac{\partial \mathcal{H}}{\partial \mathbf{m}} \right)^T \mathbf{m} \cdot \partial + \mathcal{H} \partial^T - \frac{\mathbf{B}^T}{\rho} \mathbf{B} \cdot \partial & \frac{\partial \mathcal{H}}{\partial \mathcal{E}} \mathbf{m} \cdot \partial & \left(\frac{\partial \mathcal{H}}{\partial \mathbf{B}} \right)^T \mathbf{m} \cdot \partial - \frac{\mathbf{B} \cdot \mathbf{m}}{\rho} \partial^T - \frac{\mathbf{m}^T \mathbf{B} \cdot \partial}{\rho} \\ -\frac{\mathbf{B} \cdot \partial - \mathbf{m} \mathbf{B} \cdot \partial}{\rho^2} & \frac{\mathbf{B} \otimes \partial - \mathbf{B} \cdot \partial}{\rho} & \mathbf{0} & \frac{\mathbf{m} \cdot \partial - \mathbf{m} \partial^T}{\rho} \end{pmatrix}$$

Seven eigenvalues: 2 slow and 2 fast acoustic waves, 2 Alfvén waves and 1 material wave

Weak formulation

Rewriting the system as $\mathbf{R}(\mathbf{w}) = 0$, in which

$$\mathbf{R}(\mathbf{w}) := \frac{\partial \mathbf{w}}{\partial t} + \nabla \cdot \underline{\mathbf{f}} - \nabla \cdot \underline{\mathbf{g}}, \quad \underline{\mathbf{g}} : \text{Transport process}$$

Weak formulation

$$\int_{\Omega_{x,h}} \mathbf{R}(\mathbf{w}) \cdot \mathbf{w}^* = 0, \quad \forall \mathbf{w}^* \in \vec{\mathcal{W}}_h(\Omega_{x,h})$$

Divergence free constraint

Vector potential formulation

$$\mathbf{B} = \nabla \times \mathbf{A} \quad \text{Coulomb gauge : } \nabla \cdot \mathbf{A} = 0$$

$(\nabla \cdot \mathbf{A})(\nabla \cdot \mathbf{A}^*)$ added as a penalization term

It comes to add a contribution

$$\int_{\Omega_{x,h}} \mathbf{R}(\mathbf{w}) \cdot \mathbf{w}^* + \int_{\Omega_{x,h}} \mathbf{w}' \cdot (\underline{\mathbf{L}}^T(\mathbf{w}, \partial)) \mathbf{w}^* = 0, \quad \forall \mathbf{w}^* \in \overline{\mathbf{W}}_h(\Omega_{x,h})$$

where \mathbf{w}' is vector of subscales and $\underline{\mathbf{L}}^T(\mathbf{w}, \partial)$ is the adjoint of $\underline{\mathbf{L}}(\mathbf{w}, \partial)$
 \mathbf{w}' can be approximated by

$$\mathbf{w}' \approx \underline{\mathcal{T}}(\underline{\mathbf{L}}(\mathbf{w}, \partial) \delta \mathbf{w})$$

Several options for $\underline{\mathcal{T}}$, choice based on heuristic arguments

$$\underline{\mathcal{T}} = \alpha \frac{h_e}{2\|\mathbf{a}\|} \Rightarrow \frac{\|\frac{\partial \mathbf{x}}{\partial \zeta}\|_2}{\|\Lambda\|_\infty} \mathbb{I}$$

Stabilized weak formulation

Set of interpolated variables

$$\mathbf{w} = \begin{pmatrix} \rho \\ \mathbf{m} \\ \mathcal{E} \\ \mathbf{B} \end{pmatrix} = \begin{pmatrix} \rho \\ \frac{\rho \mathbf{v}}{\gamma - 1} + \frac{1}{2} \mathbf{v} \cdot \mathbf{v} + \frac{1}{2} \mathbf{B} \cdot \mathbf{B} \end{pmatrix} \Rightarrow \mathbf{Y} = \begin{pmatrix} \rho \\ \mathbf{v} \\ T \\ \mathbf{A} \end{pmatrix}$$

Stabilized weak formulation

$$\begin{aligned} & \int_{\Omega_{x,h}} (\underline{\mathbf{M}}(\mathbf{Y}) \partial_t \mathbf{Y}) \cdot \tilde{\mathbf{w}}^* - \int_{\Omega_{x,h}} \underline{\mathbf{F}} : (\partial \odot \mathbf{w}^*) + \int_{\Omega_{x,h}} \underline{\mathbf{D}} : (\partial \odot \mathbf{w}^*) - \frac{1}{\epsilon} \int_{\Omega_{x,h}} (\nabla \cdot \mathbf{A})(\nabla \cdot \mathbf{A}^*) \\ & + \int_{\partial \Omega_{x,h}} \underline{\mathbf{F}} : (\mathbf{n} \odot \mathbf{w}^*) - \int_{\partial \Omega_{x,h}} \underline{\mathbf{D}} : (\mathbf{n} \odot \mathbf{w}^*) - \frac{1}{\epsilon} \int_{\partial \Omega_{x,h}} (\mathbf{n} \times \partial_t \mathbf{A}) \cdot \mathbf{B}^* + \frac{1}{\epsilon} \int_{\partial \Omega_{x,h}} \mathbf{S}(\mathbf{w}, \mathbf{w}_b, \mathbf{w}^*) \\ & = - \int_{\Omega_{x,h}} (\underline{\mathbf{L}}(\mathbf{w}, \partial) \delta \mathbf{w}) \cdot \underline{\mathcal{T}}(\underline{\mathbf{L}}^T(\mathbf{w}, \partial)) \mathbf{w}^* \end{aligned}$$

Stabilized weak form

In the previous equation

$$\underline{\mathbf{F}} = \begin{pmatrix} \rho \mathbf{v} \\ \rho \mathbf{v} \otimes \mathbf{v} + P\mathbf{I} - \mathbf{B} \otimes \mathbf{B} \\ \rho \mathcal{H} \mathbf{v} - \mathbf{B} \cdot \mathbf{v} \mathbf{B} \\ -\mathbf{v} \times \mathbf{B} \end{pmatrix}, \quad \underline{\mathbf{D}} = \begin{pmatrix} \underline{\mathcal{D}} \partial \rho' \\ \underline{\tau} \\ \underline{\tau} \mathbf{v} \\ -(\mathbf{E} + \mathbf{v} \times \mathbf{B}) \end{pmatrix}$$

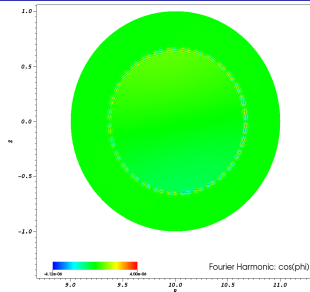
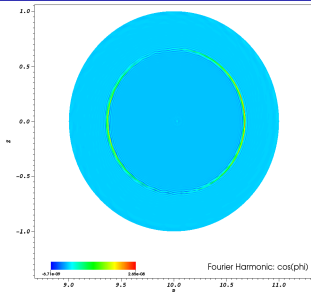
and the boundary conditions

$$\mathbf{S}(\mathbf{w}, \mathbf{w}_b, \mathbf{w}^*) = \begin{pmatrix} (\rho - \rho_b) \rho^* \chi_\rho \\ \rho(\mathbf{v} - \mathbf{v}_b) \cdot \mathbf{m}^* \chi_{\mathbf{v}} + (\rho \mathbf{v} - \mathbf{m}_b) \cdot \mathbf{m}^* \chi_m \\ \rho(T - T_b) \mathcal{E}^* \chi_T + (\rho - \rho_b) \mathcal{E}^* \chi_\rho \\ (\mathbf{A} - \mathbf{A}_b) \cdot \mathbf{J}^* \chi_{\mathbf{A}} + (\mathbf{B} - \mathbf{B}_b) \cdot \mathbf{B}^* \chi_{\mathbf{B}} \end{pmatrix}$$

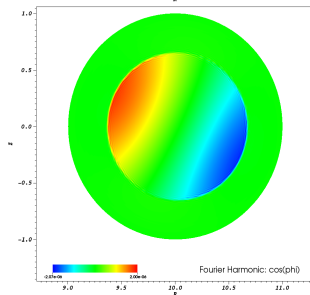
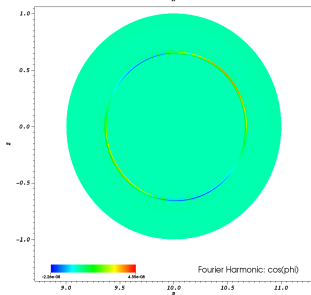
For further details, please refer to the Research Report: hal.inria.fr/hal-01294788

Resistive internal kink

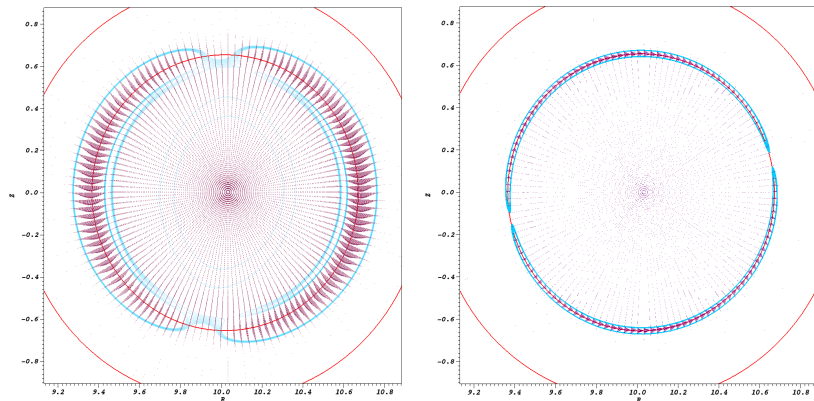
Numerical
viscosity



VMS-
Stabilization



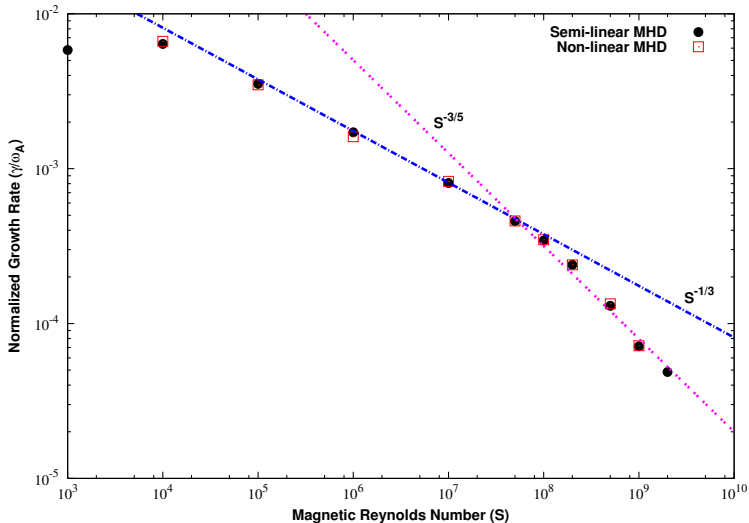
Resistive internal kink dynamics



Structure layer: $S = 10^5 \approx 10^{-1}$ and $S = 10^8 \approx 2 \cdot 10^{-2}$

$S \propto \eta^{-1}$: Magnetic Reynolds number.

Resistive internal kink: growth rate



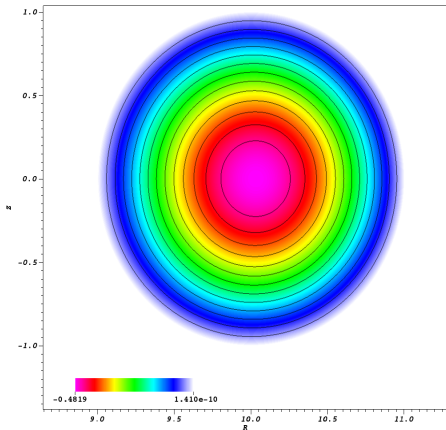
$$\gamma \propto S^{-1/3} \rightarrow \text{Kink}$$

$$\gamma \propto S^{-3/5} \rightarrow \text{Tearing}$$

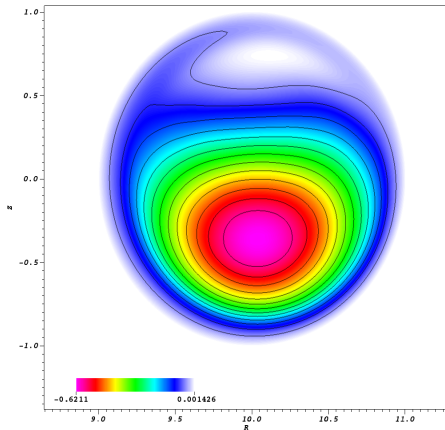
$$\text{Threshold} \approx S = 10^8$$

Resistive internal kink: magnetic reconnection

$t = 0\tau_A$

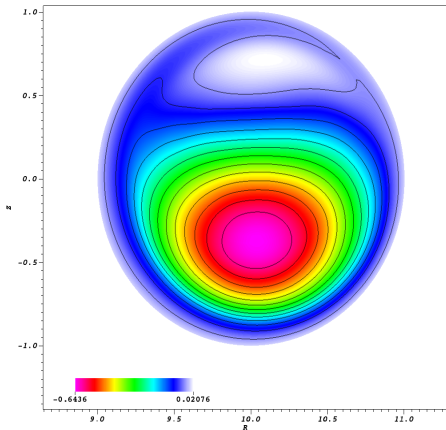


$t = 4400\tau_A$

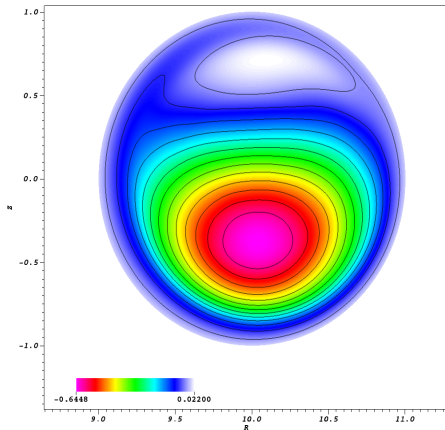


Resistive internal kink: magnetic reconnection

$t = 4460\tau_A$

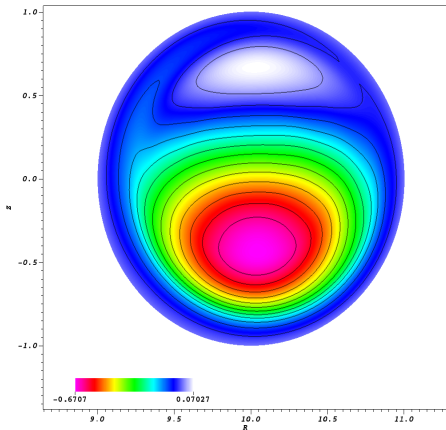


$t = 4464\tau_A$

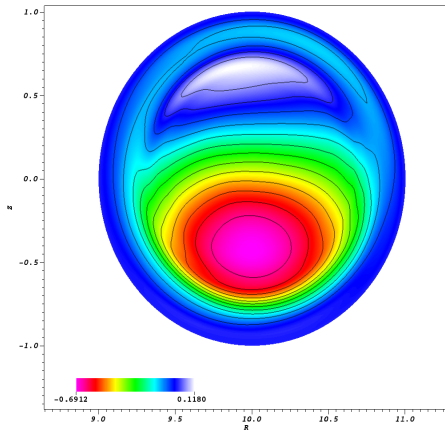


Resistive internal kink: magnetic reconnection

$t = 4648\tau_A$



$t = 5484\tau_A$



Boundary Conditions: Bohm

We need to compute the following integrals at the boundary

$$- \int_{\partial\Omega_{x,h}} \pm \rho \frac{\sqrt{\gamma T}}{\|\mathbf{B}\|} \mathbf{B} \cdot \mathbf{n} \rho^*,$$

$$- \int_{\partial\Omega_{x,h}} \left(\pm \rho \mathbf{v} \frac{\sqrt{\gamma T}}{\|\mathbf{B}\|} \mathbf{B} \cdot \mathbf{n} \right) \cdot \mathbf{m}^*,$$

$$- \int_{\partial\Omega_{x,h}} \pm (\rho \mathbf{n} + \pi \mathbf{n} - \mathbf{B}(\mathbf{B} \cdot \mathbf{n})) \cdot \mathbf{m}^*$$

$$- \int_{\partial\Omega_{x,h}} \pm p \frac{\sqrt{\gamma T}}{\|\mathbf{B}\|} \mathbf{B} \cdot \mathbf{n} \mathcal{E}^*$$

Where \mathbf{n} is the outward normal
and

$$\pm \equiv \frac{\mathbf{B} \cdot \mathbf{n}}{\|\mathbf{B} \cdot \mathbf{n}\|}$$

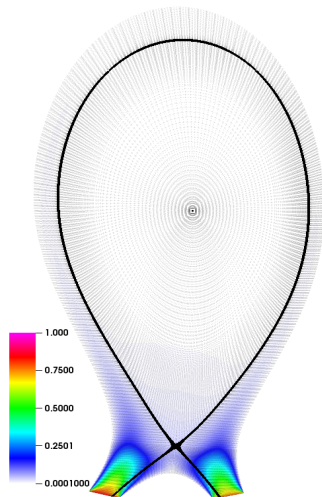
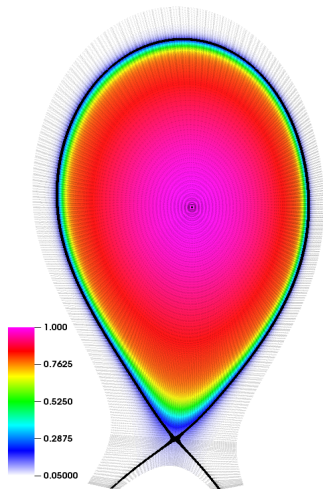
so that $\mathbf{v}_b \cdot \mathbf{n}$ is always positive

Also, a penalization term

$$\frac{1}{\epsilon} \int_{\partial\Omega_{x,h}} \left(\rho \mathbf{v} \mp \rho \sqrt{\gamma T} \frac{\mathbf{B}}{\|\mathbf{B}\|} \right) \cdot \mathbf{m}^*$$

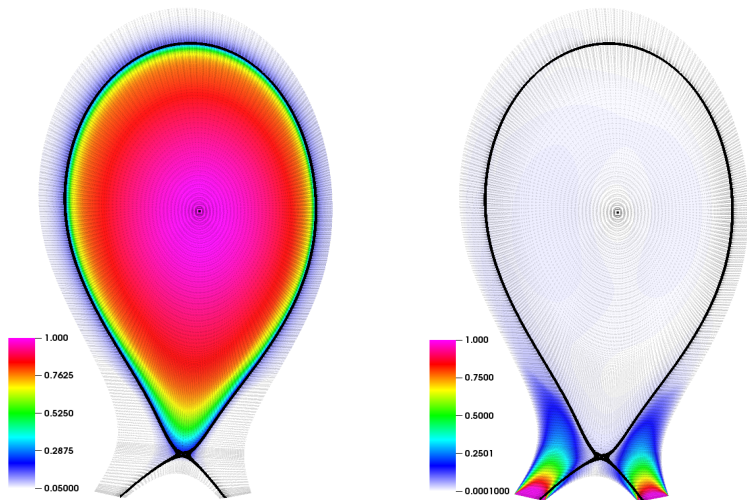
X-point results: Initial density and velocity

$t = 1\tau_A$



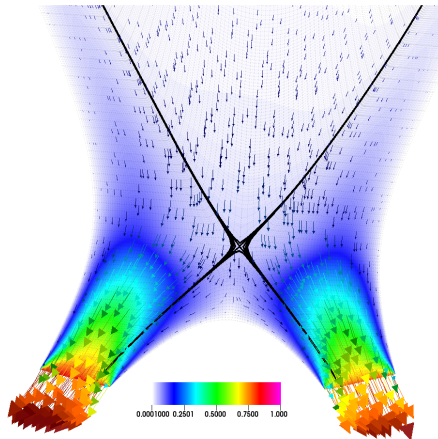
X-point results: Initial density and velocity

$t = 400\tau_{\Delta}$

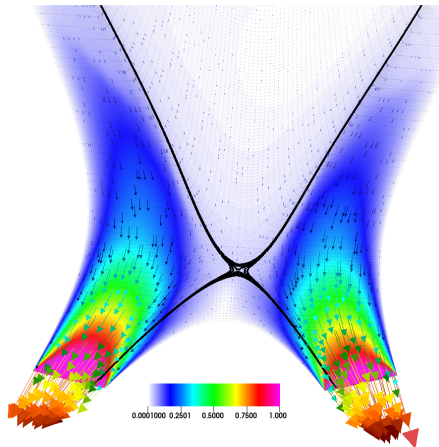


X-point results: Velocity field

$t = 1\tau_A$

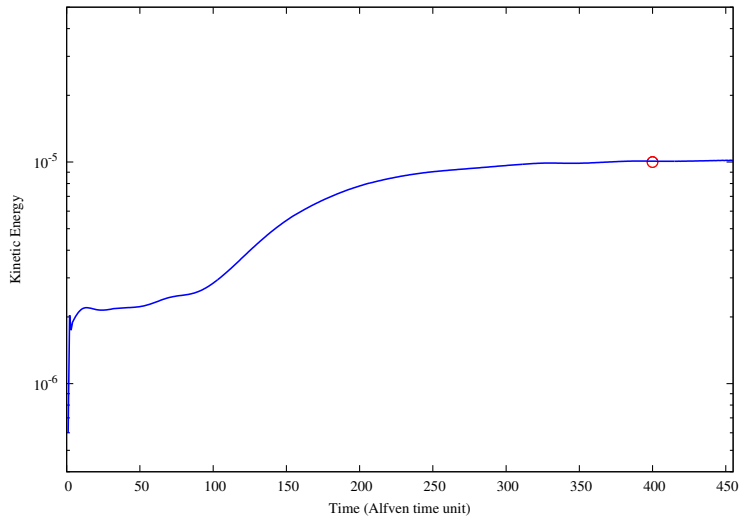


$t = 400\tau_A$



X-point results: Quasi-steady state

Evolution of the Kinetic Energy: $n = 0$



Conclusions

- Full MHD equations successfully implemented for simulating **circular** plasmas
- Stabilization scheme has improved the quality of the results
- Quasi-steady state for X-point geometry with Bohm B.C.

Perspectives

- Simulation of ELMs using the full model